RESEARCH

A laser-based sensor for selective detection of benzene, acetylene, and carbon dioxide in the fingerprint region

Mhanna Mhanna[1] · Mohamed Sy[1] · Ali Elkhazraji[1] · Aamir Farooq[1]

Abstract
The long-wavelength infrared region provides opportunities for selective and sensitive measurements in various gas-sensing applications. In this work, a mid-infrared laser-based sensor is designed and demonstrated for trace detection of benzene, acetylene, and carbon dioxide at ambient conditions. The sensor is based on a distributed-feedback quantum cascade laser emitting near 14.84 μm. Scanned-wavelength absorption spectroscopy and a multidimensional linear regression algorithm were employed to enable selective measurements of the target species. The laser wavelength was scanned over 673.8–675.1 cm^{-1} by a sine-wave injection current at 1 kHz repetition rate. Noise-limited absorbance measurement was used to calculate minimum detection limits of 0.22, 5.92, and 8.32 ppm for benzene, acetylene, and carbon dioxide, respectively, at a laser path length of 26 cm. The current measurements are limited to mixtures prepared in the lab to demonstrate the superiority of this long wavelength region for high sensitivity and interference-free multi-species measurements. Future work will apply this sensor in field measurements.

1 Introduction

In light of global warming and its ever-increasing effects on climate change, stringent regulations have been put in place to minimize greenhouse gas emissions, particularly CO_2. In addition, local pollutants, such as volatile organic compounds (VOCs) and nitric oxides (NOx), negatively impact the environment [1, 2]. Such emissions are mainly produced from various anthropogenic sources, such as industrial activity and transportation [3]. VOCs play a critical role in atmospheric reactions that lead to the formation of secondary pollutants [1]. VOCs can be toxic even at trace levels, thus monitoring their emission and abundance in workplaces and in the atmosphere is of vital importance. For instance, the 8-h time-weighted average exposure limit of some VOCs can be as low as a few ppb [4]. Therefore, extensive efforts have been directed toward developing gas sensors capable of measuring such pollutants with high sensitivity and selectivity.

Multiple techniques and devices exist for monitoring pollutants in ambient air. Examples of such devices include Fourier-transform infrared spectrometers (FTIR), photoionization detectors (PIDs), amperometric sensors, and gas chromatography (GC). Most of these devices are bulky, require sampling, long measurement time, and operation by trained personnel [5]. Furthermore, their performance can be compromised by multiple environmental factors, such as wind velocity, humidity, and temperature [5, 6]. Laser-based sensors are a better alternative for air quality monitoring on multiple fronts. These are portable, non-intrusive, have a high spectral, spatial, and temporal resolution, and are capable of measuring multiple species at once. Laser-based sensors can thus overcome many of the limitations associated with other speciation techniques [7]. Given these advantages, laser-based sensors have garnered attention from researchers and have been proven to be a useful tool for quantitative analysis of gaseous species in numerous fields, such as chemical analysis [8], monitoring of agricultural

✉ Aamir Farooq
aamir.farooq@kaust.edu.sa

Mhanna Mhanna
mhanna.mhanna@kaust.edu.sa

Mohamed Sy
mohamed.sy@kaust.edu.sa

Ali Elkhazraji
aliabdelshafi.khazraji@kaust.edu.sa

1　Mechanical Engineering Program, Physical Science and Engineering Division, Clean Combustion Research Center, King Abdullah University of Science and Technology (KAUST), 23955-6900 Thuwal, Saudi Arabia

emissions [9], control of industrial processes [10], breath analysis [11], pollution monitoring [12], and combustion diagnostics [13–16].

Infrared laser absorption spectroscopy (IR-LAS) exploits vibrational and rotational energy modes of molecules and can thus provide species-specific detection in a multitude of applications. In particular, the mid-infrared (MIR) region contains the fundamental vibrational bands of most of the atmospheric species and VOCs (e.g., CO_2, H_2O, hydrocarbons, etc.) [17, 18]. The absorption coefficients of these species are orders of magnitude stronger in this region than in the near-infrared region [19]. A specifically interesting region in the MIR is the long wavelength MIR region (LW-MIR, 13–20 µm) includes strong bending vibrational modes of many air pollutants and the C–halogen stretching modes of most halocarbons [20]. Probing molecules in this spectral region benefits from the distinct molecular features of that region, which come from the highly intense and unique absorption coefficients of the CH bending modes of many species of interest. For instance, BTEX (benzene, toluene, ethylbenzene, and xylene isomers) show overlapping absorption features over most of the IR range, which necessitates the use of advanced post-processing techniques, such as neural networks, in order to selectively measure BTEX species [4]. However, due to the distinct spectral features in the molecular fingerprint region, traditional scanned-wavelength absorption spectroscopy and simpler post-processing methods, such as multidimensional linear regression, would be sufficient for selective BTEX detection.

Despite recent advances in laser technology (e.g., telecommunications lasers, inter-band cascade lasers, quantum cascade lasers (QCLs), and frequency combs) access to the long-wavelength IR region (> 13 µm) has been limited. This, in turn, hindered the development of laser-based sensors in that highly interesting region [20]. This limitation, combined with the aforementioned advantages of this spectral region, motivated researchers to use nonlinear conversion processes, such as difference-frequency generation (DFG) and optical parametric oscillation (OPO), to access such deep wavelengths in the IR region [21, 22]. For instance, DFG has been used to probe benzene by accessing its v_4 band (Herzberg's numbering) near 14.84 µm [23, 24] and HCN by accessing its v_2 band near 14 µm [25]. However, such non-linear conversion techniques are complicated and involve bulky setups, which defies some of the main benefits of laser-based sensors.

Recently, long-wavelength distributed feedback (DFB) QCLs, fabricated via molecular beam epitaxy from the InAs/AlSb material family at Montpellier University, have been commercialized by *mirSense* (*uniMir* lasers). These are the first and only semiconductor lasers that operate in the continuous wave (cw) mode at room temperature in the long wavelength mid-infrared region (10–17 µm) [26].

This technology opens a new horizon in laser-based sensing in the long-wavelength MIR region. Karhu et al. [27] utilized the newly developed DFB-QCL to demonstrate an ultra-sensitive benzene sensor that probed its v_4 band near 14.84 µm by making use of cantilever-enhanced photoacoustic spectroscopy (CEPAS). The achieved detection limit of the CEPAS sensor was 450 ppt at a long averaging time of 200 min. Recently, Ayache et al. used the same QCL technology to develop their own benzene sensor that probed the same band (v_4) using quartz-enhanced photoacoustic spectroscopy (QEPAS) [28]. They successfully achieved a detection limit of 4 ppb at 2 min of averaging time. Shortly after, Karhu and Hieta improved their CEPAS sensor [27] by adding an adsorption enrichment stage, where benzene was collected on a sorbent and then detected from the enriched samples using photoacoustic spectroscopy [29]. This enrichment stage improved the detection limit and averaging time of their sensor to 150 ppt in 30 min (vs. 450 ppt in 200 min in their previous study [27]).

While photoacoustic spectroscopy (PAS) has several advantages, such as high sensitivity and small sample volume, it is more complex and less robust than direct, single-pass, tunable diode laser absorption spectroscopy (TDLAS). PAS is typically used in extractive sampling applications since a separate photoacoustic gas cell is required. Furthermore, photoacoustic detection elements are typically impacted when operating in harsh environments, e.g., by temperature variations, mechanical vibration, external acoustic noise, and humidity [7]. Indeed, as water–vapor affects the relaxation time of detected molecules, the previously reported QEPAS-based benzene sensor [28] was found to be heavily affected by relative humidity. Thus, it was concluded that it might be necessary to measure the relative humidity of the measured sample and apply a correction to the measured benzene concentration accordingly [27–29]. Finally, a recent review by Fathy et al. [30] concluded that direct absorption spectroscopy outperforms photoacoustic spectroscopy in terms of sensitivity at such long IR wavelengths for low-to-medium-power lasers (< 1 W, which is the case for almost all cw lasers in the IR region).

Herein, we report the development of a multispecies laser-based sensor for the detection of benzene (C_6H_6), acetylene (C_2H_2), and carbon dioxide (CO_2) near 14.84 µm. The sensor is based on scanned-wavelength direct absorption spectroscopy using a DFB-QCL tuned over 673.8–675.1 cm^{-1} and probing ro-vibrational transitions of the v_4, v_5, and v_2 bands of C_6H_6, C_2H_2 (C–H bending), and CO_2 (O–C–O bending), respectively. These species were carefully chosen to showcase the potential of laser-based sensing in the fingerprint region, as it is practically unfeasible to probe these species simultaneously using a single laser elsewhere in the IR region with reasonable sensitivity. Furthermore, the probed bands of C_6H_6 and C_2H_2 are the most intense

bands of these species in the IR. There have been extensive efforts to measure these species using laser-based sensors by probing various spectral regions [23, 31, 32]. The current measurements are limited to mixtures prepared in the lab to validate the capability of our sensor to measure benzene, acetylene, and carbon dioxide simultaneously at this newly accessible wavelength range. Future work will focus on packaging the sensor for field testing as well as improving its sensitivity using an optical cavity. Although this work is aimed at demonstrating a sensor at ambient conditions for air quality monitoring, the simultaneous detection of these species could be useful in several other applications. For example, time-resolved measurements of these species at high temperatures in combustion environments could be useful for the validation and refinement of chemical kinetic models [33, 34] and the investigation of soot formation phenomena. To our knowledge, this work represents the first demonstration of room temperature, cw-laser-based interference-free sensing of benzene, acetylene, and carbon dioxide near in the long-wavelength mid-IR spectral region.

2 Methodology

2.1 Beer–Lambert law

When a laser beam propagates through an absorbing medium, its intensity attenuation is a function of the temperature, pressure, and the concentration of the absorber. The change in laser intensity is given by the Beer–Lambert law [35]:

$$\alpha_\nu = -ln\left(\frac{I_t}{I_0}\right) = \sigma(T, P, \nu) \cdot n \cdot L \tag{1}$$

where α_ν is the absorbance at frequency ν, I_t and I_0 are the transmitted and incident laser intensities, respectively, $\sigma(T, P, \nu)$ is the temperature- and pressure-dependent absorption cross section of the absorber at frequency ν, n is the number density of the absorbing gas, and L is the path of the laser through the absorbing medium. When multiple species absorb at the same frequency, their absorbance is simply added to obtain the total composite absorbance of the mixture. The number density is a direct function of the mole fraction of the absorbing species, χ:

$$n = \frac{N}{V} = \frac{P \cdot \chi}{k_B \cdot T} \tag{2}$$

where N is the total number of absorbers in the mixture, V is the volume of the sampling cell, and k_B is the Boltzmann constant. By combining Eqs. (1) and (2), absorbance can be directly related to mole fraction of the absorbing species, as follows:

$$\alpha_\nu = \frac{\sigma(T, P, \nu) \cdot P \cdot L \cdot \chi}{k_B \cdot T} \tag{3}$$

The uncertainty in the measured absorbance results from changes in the incident and transmitted intensities of the laser:

$$\frac{\delta\alpha_\nu}{\alpha_\nu} = \sqrt{\left(\frac{\delta I_t}{I_t}\right)^2 + \left(\frac{\delta I_0}{I_0}\right)^2} \tag{4}$$

All measurements reported here were carried out at ambient conditions with temperature and pressure uncertainties of 0.03% and 0.12% of the readings, respectively. Absorption cross sections are reported to have 1.66% uncertainty [36] and the optical path length is known with an uncertainty of < 1%. The absorbance uncertainty, as calculated from the fluctuation in the absorbance signal, is ∼ 0.1%. Hence, the measured mole fraction of the absorbing species has a calculated uncertainty of ∼3% according to Eq. (5).

$$\frac{\delta\chi}{\chi} = \sqrt{\left(\frac{\delta\alpha_\nu}{\alpha_\nu}\right)^2 + \left(\frac{\delta\sigma}{\sigma}\right)^2 + \left(\frac{\delta P}{P}\right)^2 + \left(\frac{\delta T}{T}\right)^2 + \left(\frac{\delta L}{L}\right)^2} \tag{5}$$

2.2 Wavelength selection

Benzene has absorption bands in the ultraviolet (UV) spectrum. However, a multitude of other hydrocarbons in the UV range interfere with benzene measurements. Highly selective detection of benzene and other air pollutants, such as acetylene and CO_2, is more feasible in the infrared (IR) region. Benzene has ten non-degenerate and ten doubly degenerate vibrational motions. The strongest wavelength to measure benzene in the IR is near 674 cm^{-1} (14.837 μm), which corresponds to the C–H bending motion. While this band is generally referred to as the ν_4 band of benzene, we highlight that it is sometimes called ν_{11} due to different numbering conventions [37]. Here, we will refer to this band as ν_4. The absorption cross-section at the peak of the Q-branch of the ν_4 band is ∼ 80 times larger than the widely accessible C–H stretch band near 3.3–3.4 μm, and ∼ 5 times larger than the peak in the UV range [38]. The normalized absorption cross sections of benzene, acetylene, and carbon dioxide are shown in Fig. 1a, as determined from the Pacific Northwest National Laboratory (PNNL) and HITRAN databases [36, 39]. Figure 1b shows a close-up view of the cross-sections near 14.84 μm. Previous benzene sensing works were conducted near 1038 cm^{-1} (9.64 μm) [12], 3040 cm^{-1} (3.29 μm) [40], and 3090 cm^{-1} (3.4 μm) [41]. However, these sensors will be prone to high uncertainty due to the absorption interference from ozone, isoprene, and other TEX species (toluene, ethylbenzene, and xylene isomers).
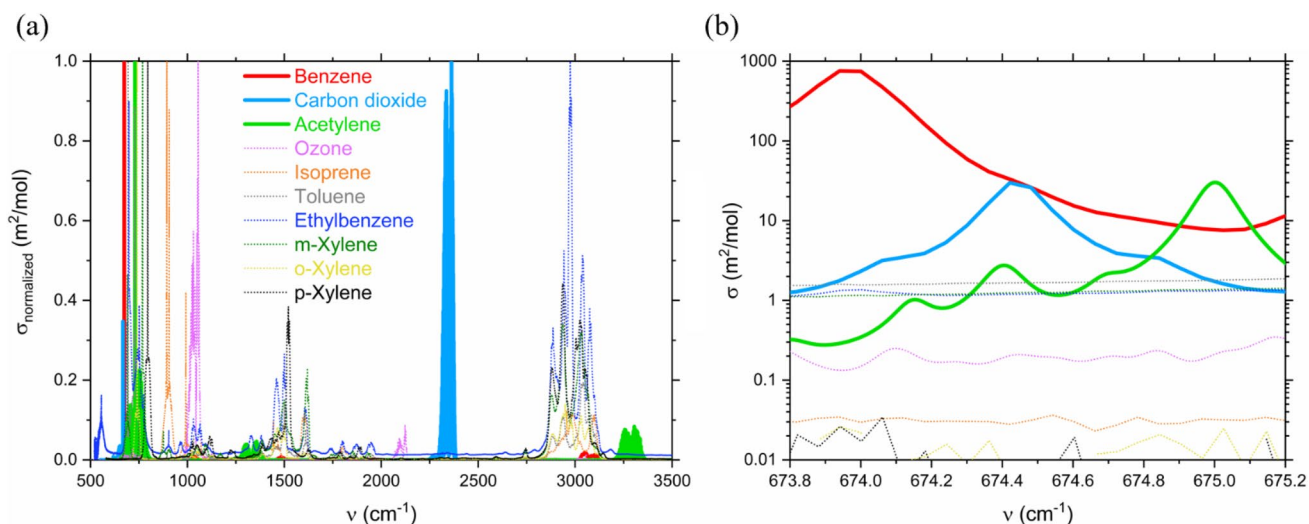
(a)

(b)

Fig. 1 a Normalized absorption cross sections of benzene, carbon dioxide, acetylene, ozone, isoprene, toluene, ethylbenzene, and xylene isomers at $T = 298$ K and $P = 1$ atm. Acetylene and ozone cross sections were simulated using [39], while the rest were simulated using [36]. **b** Zoom-in view of the selected wavelength region

In addition to being the strongest ro-vibrational band of benzene, the ν_4 band contains a narrow benzene feature (Q-branch) near 673.973 cm^{-1} with HWHM = 0.12 cm^{-1}, which enhances the selectivity of benzene sensing. Therefore, we selected a benzene probe wavelength near 673.973 cm^{-1} (14.84 μm) in the ν_4 band. Figure 1b shows that ozone, isoprene, and TEX absorbance values are negligible in this wavelength range as compared to benzene (note that the y-axis is a log scale). The low resolution of the displayed spectra is because of the spectral resolution of the FTIR used to acquire the PNNL database [36]. The selected wavelength range, however, has some spectral overlap between benzene, acetylene, and carbon dioxide. Although the ν_4 band has been targeted previously for benzene detection [24, 27–29, 38], spectral interference from CO_2 was not addressed, which can be significant at trace benzene concentrations. In this work, a multi-dimensional linear regression (MLR) algorithm, discussed in Sect. 2.2, is implemented to simultaneously measure benzene, acetylene, and CO_2.

2.3 Multidimensional linear regression

Due to the spectral overlap between our target species, particularly between benzene and CO_2, over 673.8–675.2 cm^{-1}, a multidimensional linear regression (MLR) algorithm is utilized to untangle the composite absorbance spectrum into contributions from individual target species. Assuming that the absorption from interfering species is negligible, the measured spectrum can then be considered to be a linear combination of three reference spectra of the target species [42]:

$$\alpha_\nu = \sum_{i=1}^{3} c_i \cdot r_{i,\nu}. \tag{6}$$

where α_ν represents the measured composite absorbance at frequency ν and c_i is the contribution of each species to the total absorbance, where $i = 1$, 2, and 3 correspond to benzene, acetylene, and CO_2, respectively. $r_{\nu,i}$ corresponds to the reference absorbance value of the i th species at frequency ν. In vector form, the equation is:

$$\begin{pmatrix} \alpha_1 \\ \alpha_2 \\ \vdots \\ \alpha_n \end{pmatrix} = c_{benzene} \begin{pmatrix} r_{1,benzene} \\ r_{2,benzene} \\ \vdots \\ r_{n,benzene} \end{pmatrix} + c_{acetylene} \begin{pmatrix} r_{1,acetylene} \\ r_{2,acetylene} \\ \vdots \\ r_{n,acetylene} \end{pmatrix}$$
$$+ c_{CO_2} \begin{pmatrix} r_{1,CO_2} \\ r_{2,CO_2} \\ \vdots \\ r_{n,CO_2} \end{pmatrix}$$

$$\tag{7}$$

A least squares solution provides the contribution (c_i) of each species (i) to the measured composite absorbance spectrum (α_ν) for given reference spectra of each species ($r_{\nu,i}$).

Here, $r_{\nu,i}$ is $m \times 3$ matrix, c_i is unknown 1-D vector with a length of 3, and α_ν is 1-D measured absorbance vector of length m, such that $m > 3$. This results in m equations with 3 unknowns, and thus the obtained linear system of

equations is not exact. Therefore, the resulting coefficients correspond to the least squares solution rather than an exact solution. The least squares solution deconvolutes the composite measured absorbance vector, α_v, into contributions of each absorbing species, c_i, with respect to each reference vector of these species, $r_{v,i}$. For example, suppose that the reference spectra of benzene and carbon dioxide are obtained from the PNNL database at 100 ppm [36], and the reference spectrum of acetylene is obtained from the HITRAN database at 100 ppm [39]; if the least squares solution provides the coefficients of 0.5, 1, and 2, then this means that the deduced concentrations of benzene, acetylene, and carbon dioxide are 50 ppm, 100 ppm, and 200 ppm, respectively. The distinct absorption features of the target species in the chosen long-wavelength IR region facilitate accurate determination of the least squares solution.

2.4 Optical setup

The proposed sensor uses a continuous-wave quantum cascade laser (cw-QCL, *mirSense*) emitting near 14.84 μm with an output power of ~ 4 mW. This QCL is the first semiconductor laser that emits cw long-wavelength mid-IR radiation without requiring cryogenic cooling [27]. The laser is enclosed in a sub-mount with a PT100 temperature sensor and a Peltier cooler, and placed on a water-cooled aluminum plate. We prepared test gas mixtures by mixing grade 5 nitrogen with high-purity benzene (99.8%, Sigma-Aldrich), acetylene (99.9%, AHG), and CO_2 (99.995%, Air Liquide). Benzene was measured at the Q-branch of the v_4 band at 673.973 cm^{-1}, acetylene was measured at 675.05 cm^{-1}, and CO_2 was measured at 674.45 cm^{-1}. As Fig. 1b shows, these targeted peak wavelengths have interference absorption from other species which was overcome using the MLR algorithm. The laser wavelength was tuned

over 673.8–675.15 cm^{-1} by a sine-wave injection current (1 kHz scan rate) and a 7.62 cm Fabry–Pérot Germanium etalon (FSR = 0.0163 cm^{-1}) was utilized to convert the scan time to wavenumbers. Figure 2 shows the schematic of the sensor. Two ZnSe windows (Thorlabs) were mounted on a 26-cm gas sampling cell. The transmitted signal was collected using a liquid-nitrogen-cooled HgCdTe photodetector.
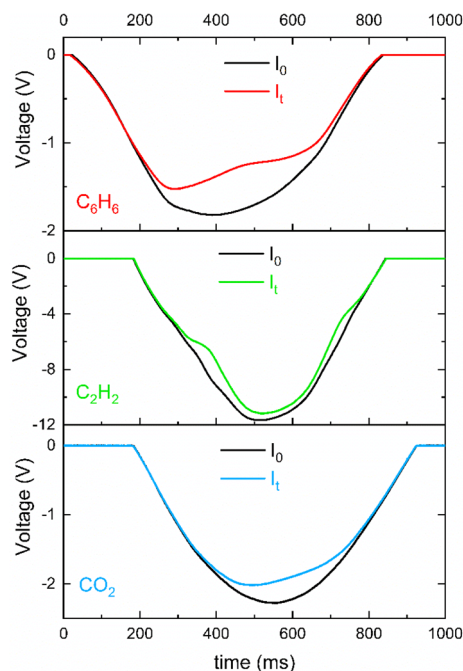
Fig. 3 Incident and transmitted laser intensities recorded by the photodetector. Measured mole fractions of benzene, acetylene, and carbon dioxide are 48, 794, and 511 ppm, respectively. $T = 298$ K, $P = 1$ atm, and $L = 26$ cm
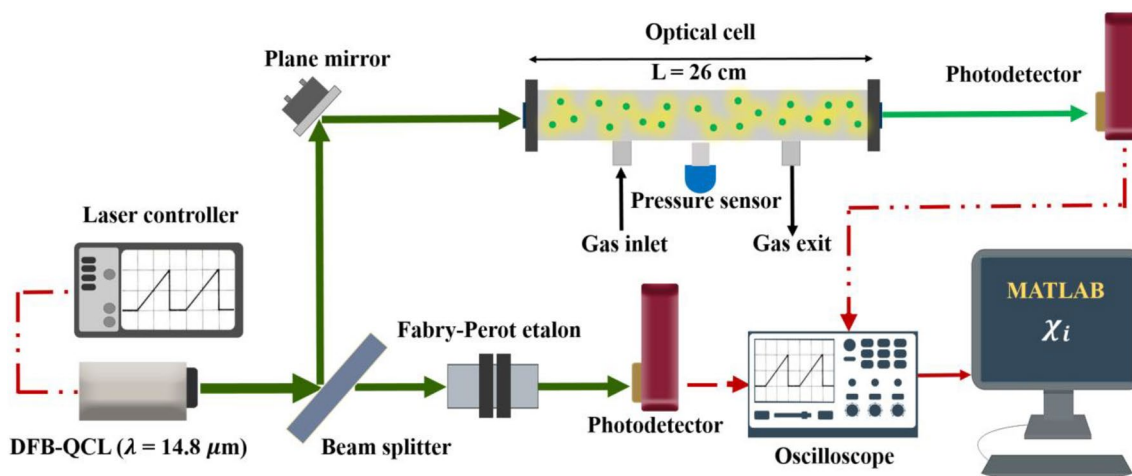
Fig. 2 Optical schematic of the sensor

3 Experimental results

3.1 Absorbance measurement

Figure 3 shows examples of the incident (I_0) and transmitted (I_t) laser intensity signals. The panels correspond to 48, 511, and 794 ppm of benzene, carbon dioxide, and acetylene, respectively, mixtures in nitrogen. Equation (1) was used to transform these intensity signals into the absorbance spectra shown in Fig. 4. Good agreement was found between the measured and simulated (using PNNL and HITRAN databases) absorbance at $T = 298$ K, $P = 1$ atm, and $L = 26$ cm. The simulated mole fractions of benzene, acetylene, and carbon dioxide are 50, 790, and 510 ppm, while the measured ones are 48, 794, and 511 ppm, respectively. The PNNL database suffers from a relatively low spectral resolution with a linewidth of 0.1 cm^{-1}. The narrow linewidth (< 0.006 cm^{-1}) of our QCL allows us to better resolve the absorption spectra of benzene and carbon dioxide, which clarified the peak of the strongest absorption feature of benzene in the IR region.

3.2 Sensor validation using multispecies mixtures

Gas samples containing benzene, acetylene, and carbon dioxide were prepared and multidimensional linear regression (MLR) was applied to deduce the mole fraction of each target species from the composite measured absorbance spectra. In these mixtures, benzene mole fraction was varied over 0–250 ppm, while the mole fractions of acetylene and carbon dioxide were both varied over 0–2000 ppm. Figure 5 shows a comparison between the measured and reference composite absorbance spectra of two manometrically prepared mixtures. Mixture A contains 50, 1300, and 1600 ppm of benzene, carbon dioxide, and acetylene, respectively, in
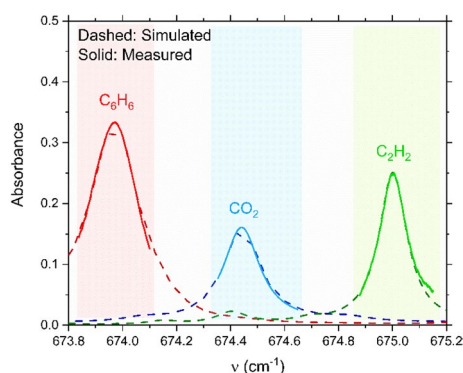
Fig. 5 Measured and reference composite absorbance spectra of mixtures A and B at $T = 298$ K and $P = 1$ atm. The bottom panel shows the residual between the measured and reference absorbance spectra

nitrogen, while the mole fractions of these species in mixture B are 25, 800, and 1000 ppm, respectively. In addition to measurement uncertainties, residuals between the measured and reference spectra are mainly due to the low spectral resolution of the PNNL database. The discontinuities in the measured absorbance spectra are due to switching the tuning range of the laser by changing its current and temperature.

Figure 6 shows the experimentally measured mole fractions of benzene, carbon dioxide, and acetylene against manometric (known) values. The dotted line represents the linear fit, which demonstrates remarkable agreement between the measured and manometric mole fractions. The

Fig. 4 Measured and simulated absorbance spectra at $T = 298$ K, $P = 1$ atm, and $L = 26$ cm. Simulated mole fractions of benzene, acetylene, and carbon dioxide are 50, 790, and 510 ppm, respectively [36, 39]
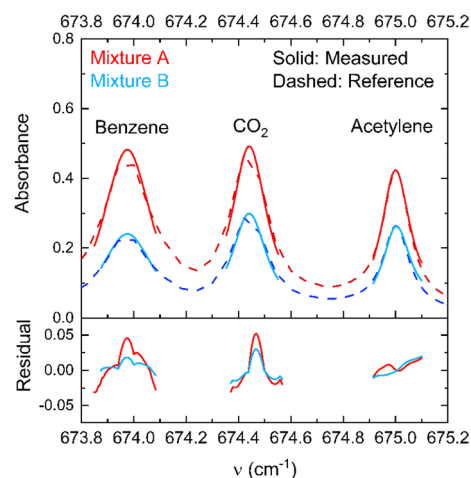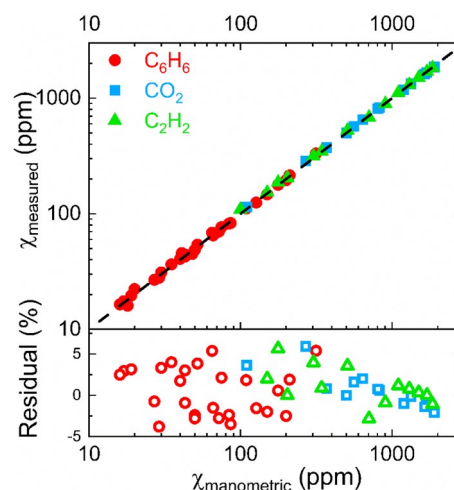
Fig. 6 Comparison of experimentally measured and manometric mole fractions of benzene, carbon dioxide, and acetylene. The dashed line represents the linear fit. The bottom panel shows the residuals between the measured and manometric mole fractions
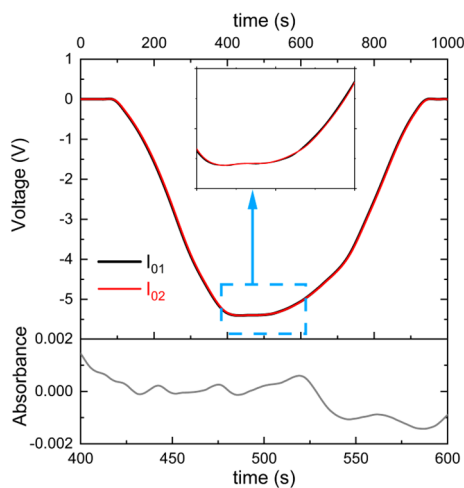
Fig. 7 Two representative incident laser intensity signals (I_0), with the inset showing a close-up view of the fluctuations in these signals

residuals of these concentrations are shown in the bottom panels of these figures. For all species, the residual is within 5% of the reading, which is in good agreement with the uncertainty of the measurements calculated using Eq. (5). The higher residual at low mole fractions is due to the multi-fold dilution process used for preparing the mixtures to reach such low mole fraction values.

3.3 Minimum detection limits

The minimum detection limit (MDL) is one of the most important parameters in gas-sensing [43]. A reasonable value of detection limit may be determined from the measured laser intensity fluctuation, which is a direct indication of the signal noise. These fluctuations arise from various noise sources, such as mechanical oscillations, etalon effects, and Johnson noise from the detector and/or the laser source. Figure 7 shows two non-absorbed laser intensity signals (I_0), with the inset showing a close-up of the fluctuations in these signals which indicates the noise level in the measured signals. We observe that 0.2% absorbance corresponds to an SNR = 1. Equation 3 was used to convert this absorption to minimum detection limits of 0.22, 5.92, and 8.32 ppm, for benzene, acetylene, and carbon dioxide, respectively. While lower MDLs exist in literature, especially for benzene, the MDL obtained here (0.22 ppm) is the lowest among single-pass sensors in literature. For example, Lewicki et al. [12] probed the benzene absorption feature near 9.64 μm to show the possibility of achieving an MDL of 12 ppb using a multi-pass cell at an averaging time of 200 s. We have previously shown that achieving an MDL of 2 ppb for benzene is

possible near 3.29 μm by in a cavity-enhanced absorption spectroscopy setup at an averaging time of 6 s [2]. Therefore, probing the ν_4 band of benzene near 14.84 μm, which is ~ 50 times stronger than the one near 3.29 μm, provides the possibility of achieving unprecedented MDL using a multi-pass cell or an optical cavity.

4 Conclusions

We have demonstrated the first room temperature, cw-laser-based interference-free sensing of benzene, acetylene, and carbon dioxide in the fingerprint wavelength region. We applied our sensor to measure the target species at ppm levels in various mixtures. Spectral resolution is improved from 0.06 cm^{-1} in the PNNL database to 0.006 cm^{-1} in these measurements. Multidimensional linear regression was applied to enable selective measurements of benzene, acetylene, and carbon dioxide. The sensor was validated using manometric mixtures prepared in the lab within a residual of 5%. Minimum detection limits of 0.22, 5.92, and 8.32 ppm were determined for benzene, acetylene, and carbon dioxide, respectively, at a laser path length of 26 cm. Such a sensor can be used for selective and sensitive detection of many species in air quality monitoring and combustion applications.

Author contributions MM wrote the manuscript, developed the codes, prepared the experimental setup, ran experiments, and processed the data. MS helped in running the experiments. AE helped in running the experiments and writing the manuscript. AF supervised the project. All authors reviewed the manuscript.

Data availability Data underlying the results presented in this paper are not publicly available at this time but may be obtained from the authors upon reasonable request.

Declarations

Conflict of interest The authors have declared that they have no competing interests.

References

1. H. Akimoto, Global air quality and pollution. Science **302**, 1716–1719 (2003)
2. M. Mhanna, G. Zhang, N. Kunnummal, A. Farooq, Cavity-enhanced measurements of benzene for environmental monitoring. IEEE Sens. J. **21**, 3849–3859 (2020)

3. M. Marć, M. Tobiszewski, B. Zabiegała, M. de la Guardia, J. Namieśnik, Current air quality analytics and monitoring: a review. Anal. Chim. Acta **853**, 116–126 (2015)

4. M. Mhanna, M. Sy, A. Arfaj, J. Llamas, A. Farooq, Laser-based selective BTEX sensing using deep neural networks. Opt. Lett. **47**, 3247–3250 (2022)

5. L. Spinelle, M. Gerboles, G. Kok, S. Persijn, T. Sauerwald, Review of portable and low-cost sensors for the ambient air monitoring of benzene and other volatile organic compounds. Sensors **17**, 1520 (2017)

6. J.E. Nyquist, D.L. Wilson, L.A. Norman, R.B. Gammage, Decreased sensitivity of photoionization detector total organic vapor detectors in the presence of methane. Am. Ind. Hyg. Assoc. J. **51**, 326–330 (1990)

7. A. Farooq, A.B. Alquaity, M. Raza, E.F. Nasir, S. Yao, W. Ren, Laser sensors for energy systems and process industries: perspectives and directions. Prog. Energy Combust. Sci. **91**, 100997 (2022)

8. R.F. Curl, F. Capasso, C. Gmachl, A.A. Kosterev, B. McManus, R. Lewicki, M. Pusharsky, G. Wysocki, F.K. Tittel, Quantum cascade lasers in chemical physics. Chem. Phys. Lett. **487**, 1–18 (2010)

9. T.J. Griffis, Tracing the flow of carbon dioxide and water vapor between the biosphere and atmosphere: a review of optical isotope techniques and their application. Agric. For. Meteorol. **174**, 85–109 (2013)

10. I. Linnerud, P. Kaspersen, T. Jaeger, Gas monitoring in the process industry using diode laser spectroscopy. Appl. Phys. B: Lasers Optics **67**, 297 (1998)

11. T.H. Risby, F.K. Tittel, Current status of midinfrared quantum and interband cascade lasers for clinical breath analysis. Opt. Eng. **49**, 111123 (2010)

12. R. Lewicki, M. Witinski, B. Li, G. Wysocki, in: Novel In-Plane Semiconductor Lasers XV, SPIE, 2016, pp. 241–247.

13. R.K. Hanson, D.F. Davidson, Recent advances in laser absorption and shock tube methods for studies of combustion chemistry. Prog. Energy Combust. Sci. **44**, 103–114 (2014)

14. A. Elkhazraji, M.K. Shakfa, M. Adil, M. Mhanna, H. Jin, M. Marangoni, B. Giri, A. Farooq, *Laser Applications to Chemical, Security and Environmental Analysis* (Optica Publishing Group, Washington, 2022), p.LM4B.3

15. M. Mhanna, M. Sy, A. Elkhazraji, A. Farooq, *Computational Optical Sensing and Imaging* (Optica Publishing Group, Washington, 2022), p.JTu2A. 4

16. M. Mhanna, M. Sy, A. Elkhazraji, A. Farooq, Deep neural networks for simultaneous BTEX sensing at high temperatures. Opt. Express **30**, 38550–38563 (2022)

17. A. Elkhazraji, M.K. Shakfa, N. Abualsaud, M. Mhanna, M. Sy, M. Marangoni, A. Farooq, Laser-based sensing in the long-wavelength mid-infrared: chemical kinetics and environmental monitoring applications. App. Optic. **62**, A46 (2023)

18. M. Mhanna, M. Sy, A. Farooq, A selective laser-based sensor for fugitive methane emissions. Sci. Rep. **13**, 1573 (2023)

19. C.S. Goldenstein, R.M. Spearrin, J.B. Jeffries, R.K. Hanson, Infrared laser-absorption sensing for combustion gases. Prog. Energy Combust. Sci. **60**, 132–176 (2017)

20. H. Timmers, A. Kowligy, A. Lind, F.C. Cruz, N. Nader, M. Silfies, G. Ycas, T.K. Allison, P.G. Schunemann, S.B. Papp, Molecular fingerprinting with bright, broadband infrared frequency combs. Optica **5**, 727–732 (2018)

21. M.K. Shakfa, M. Lamperti, R. Gotti, D. Gatti, A. Elkhazraji, K. Hakimov, M. Marangoni, A. Farooq, in: Nonlinear Frequency Generation and Conversion: Materials and Devices XX, SPIE, 2021, pp. 23–29.

22. L. Maidment, P.G. Schunemann, D.T. Reid, Molecular fingerprint-region spectroscopy from 5 to 12 μm using an orientation-patterned gallium phosphide optical parametric oscillator. Opt. Lett. **41**, 4261–4264 (2016)

23. K. Chen, B. Zhang, M. Guo, H. Deng, B. Yang, Z. Gong, W. Peng, Q. Yu, All-optical photoacoustic multigas analyzer using digital fiber-optic acoustic detector. IEEE Trans. Instrum. Meas. **69**, 8486–8493 (2020)

24. M.K. Shakfa, A. Elkhazraji, M. Marangoni, A. Farooq, Optical Sensors 2021, SPIE, 2021, pp. 166–172.

25. A. Elkhazraji, M. Adil, B. Giri, M. Mhanna, N. Abualsaud, A.A. Alsulami, M.K. Shakfa, M. Marangoni, A. Farooq, *CLEO: Applications and Technology* (Optica Publishing Group, Washington, 2022), p.ATu4I. 2

26. H. Nguyen Van, Z. Loghmari, H. Philip, M. Bahriz, A.N. Baranov, R. Teissier, Photonics, MDPI, 2019, pp. 31.

27. J. Karhu, H. Philip, A. Baranov, R. Teissier, T. Hieta, Sub-ppb detection of benzene using cantilever-enhanced photoacoustic spectroscopy with a long-wavelength infrared quantum cascade laser. Opt. Lett. **45**, 5962–5965 (2020)

28. D. Ayache, W. Trzpil, R. Rousseau, K. Kinjalk, R. Teissier, A.N. Baranov, M. Bahriz, A. Vicet, Benzene sensing by Quartz enhanced photoacoustic spectroscopy at 14.85 μm. Opt. Express **30**, 5531–5539 (2022)

29. J. Karhu, T. Hieta, Enhancement of photoacoustic spectroscopy with sorption enrichment for ppt-level benzene detection. Appl. Opt. **61**, 1892–1897 (2022)

30. A. Fathy, Y.M. Sabry, I.W. Hunter, D. Khalil, T. Bourouina, Direct absorption and photoacoustic spectroscopy for gas sensing and analysis: a critical review. Laser Photonics Rev. **16**(8), 2100556 (2022)

31. C. Wang, Z. Wang, X. Pang, Quartz-enhanced photoacoustic spectroscopy for four-component gas detection based on two off-beam acoustic microresonators. Front. Phys. **8**, 594326 (2020)

32. G. Durry, J. Li, I. Vinogradov, A. Titov, L. Joly, J. Cousin, T. Decarpenterie, N. Amarouche, X. Liu, B. Parvitte, Near infrared diode laser spectroscopy of C2H2, H2O, CO2 and their isotopologues and the application to TDLAS, a tunable diode laser spectrometer for the martian PHOBOS-GRUNT space mission. Appl. Phys. B **99**, 339–351 (2010)

33. A.O. Abdalla, D. Liu, Dimethyl carbonate as a promising oxygenated fuel for combustion: a review. Energies **11**, 1552 (2018)

34. K. Alexandrino, J. Salinas, Á. Millera, R. Bilbao, M.U. Alzueta, Sooting propensity of dimethyl carbonate, soot reactivity and characterization. Fuel **183**, 64–72 (2016)

35. D.F. Swinehart, The Beer-lambert law. J. Chem. Educ. **39**, 333 (1962)

36. S.W. Sharpe, T.J. Johnson, R.L. Sams, P.M. Chu, G.C. Rhoderick, P.A. Johnson, Gas-phase databases for quantitative infrared spectroscopy. Appl. Spec. **58**(12), 1452–1461 (2004)

37. M.K. Shakfa, M. Mhanna, H. Jin, D. Liu, K. Djebbi, M. Marangoni, A. Farooq, A mid-infrared diagnostic for benzene using a tunable difference-frequency-generation laser. Proc. Combust. Inst. **38**, 1787–1796 (2021)

38. M.K. Shakfa, M. Mhanna, M. Marangoni, A. Farooq, 2020 Conference on Lasers and Electro-Optics (CLEO), IEEE, 2020, pp. 1–2.

39. I.E. Gordon, L.S. Rothman, C. Hill, R.V. Kochanov, Y. Tan, P.F. Bernath, M. Birk, V. Boudon, A. Campargue, K. Chance, The HITRAN2016 molecular spectroscopic database. J. Quant. Spectrosc. Radiat. Transfer **203**, 3–69 (2017)

40. M. Mhanna, G. Zhang, A. Farooq, N. Kunnummal, A.J. Khamis, in, Google Patents, 2022.

41. R. Sur, Y. Ding, R. Jackson, R. Hanson, Tunable laser-based detection of benzene using spectrally narrow absorption features. Appl. Phys. B **125**, 1–8 (2019)

42. A.A. Kosterev, R.F. Curl, F.K. Tittel, C. Gmachl, F. Capasso, D.L. Sivco, J.N. Baillargeon, A.L. Hutchinson, A.Y. Cho, Effective utilization of quantum-cascade distributed-feedback lasers in absorption spectroscopy. Appl. Opt. **39**, 4425–4430 (2000)

43. F.K. Tittel, D. Richter, A. Fried, Mid-infrared laser applications in spectroscopy, in: Solid-state mid-infrared laser sources, Springer, 2003, pp. 458–529.